antibiotics

MDPI

Article

Diverse Role of *bla*CTX-M and Porins in Mediating Ertapenem Resistance Among Carbapenem Resistant Enterobacterales

Cody A. Black [1,2], Raymond Benavides [1,2], Sarah M. Bandy [1,2], Steven S. Dallas [2-4], Gerard Gawrys [1,2,4], Wonhee So [5], Alvaro G. Moreira, Samantha Aguilar [1,2,4], Kevin Quidilla [1,2], Dan F. Smelter [1,2], Kelly R. Reveles [1,2], Christopher R. Frei [1,2,4], Jim M. Koeller [1,2] and Grace C. Lee [1,2,6]*

[1] College of Pharmacy, The University of Texas at Austin, Austin, TX 78712, USA
[2] Joe R. and Teresa Lozano Long School of Medicine, The University of Texas Health at San Antonio, San Antonio, TX 78229, USA
[3] Department of Pathology and Laboratory Medicine, The University of Texas Health at San Antonio, San Antonio, TX 78229, USA
[4] University Health System, 4502 Medical Drive, San Antonio, TX 78229, USA
[5] College of Pharmacy, Western University of Health Sciences, Pomona, CA 91766, USA
[6] Veterans Administration Research Center for AIDS and HIV-1 Infection and Center for Personalized Medicine, South Texas Veterans Health Care System, San Antonio, TX 78229, USA
* Correspondence: Grace C. Lee; leeg3@uthscsa.edu

Abstract: This study investigates the emergence of ertapenem-resistant, meropenem-susceptible (ErMs) among non-carbapenemase producing (NCP) and carbapenemase producing (CP) *Escherichia coli* and *Klebsiella pneumoniae*. As mutations for ertapenem resistance establish the genetic background for non-carbapenemase meropenem resistance, there is a great need for antibiotic stewards and researchers to understand the determinants of a strain's propensity to become resistant. Whole genome sequencing was conducted on clinical carbapenem-resistant *E. coli* (CREC) and *K. pneumoniae* (CRKP) across 5 hospitals in San Antonio, U.S. from 2012-2018. The majority of carbapenem resistant Enterobacterales (CRE) were NCP (54%; 41/76). The *bla*CTX-M was found to be most prevalent among NCP isolates ($p = 0.02$). LC-MS/MS analysis of carbapenem hydrolysis revealed that *bla*CTX-M-mediated carbapenem hydrolysis, indicating the need to reappraise the term, "non-carbapenemase (NCP)" for quantitatively uncharacterized CRE strains harboring *bla*CTX-M. Antimicrobial susceptibility results showed that 56% of all NCPE isolates had an ErMs phenotype (NCPE vs. CPE, $p < 0.001$), with *E. coli* driving the phenotype (*E. coli* vs. *K. pneumoniae*, $p < 0.001$). ErMs strains carrying *bla*CTX-M, had approximately 4-fold more copies of *bla*CTX-M than ceftriaxone-resistant but ertapenem and meropenem susceptible (EsMs) isolates (3.7 v. 0.9, $p < 0.001$). ErMs also carried more mobile genetic elements (MGEs), particularly IS26 composite transposons, than EsMs (37 vs. 0.2, $p < 0.0001$). Immunoblot analysis demonstrated the absence of OmpC expression in NCP-ErMs *E. coli*, with 92% of strains lacking full contig coverage of *ompC*. Overall, this work provides evidence of a collaborative effort between *bla*CTX-M and OmpC in NCP strains that confer resistance to ertapenem but not meropenem. To thwart potential mismanagement of CRE infected patients, future efforts should focus on understanding the mechanism(s) underlying OmpC loss, developing rapid methods to detect *bla*CTX-M copy number variants, and targeted antimicrobials for NCPE and ErMs strains.

Keywords: CRE; ESBL; extended spectrum beta lactamase; non-carbapenemase-producing; ertapenem-resistant; meropenem-susceptible; porin loss; outer-membrane protein; mobile genetic elements; molecular epidemiology

Citation: Black, C.A.; Benavides, R.; Bandy, S.M.; Dallas, S.S.; Gawrys, G.; So, W.; Moreira, A.G.; Aguilar, S.; Quidilla, K.; Smelter, D.F.; et al. Diverse Role of *bla*CTX-M and Porins in Mediating Ertapenem Resistance Among Carbapenem Resistant Enterobacterales. *Antibiotics* **2024**, *11*, x. https://doi.org/10.3390/xxxxx

Academic Editor(s): Name

Received: date
Revised: date
Accepted: date
Published: date

1. Introduction

Carbapenem resistance in the Enterobacterales family poses a growing and pervasive threat to human health worldwide [1]. Despite advances in treatment strategies, these

organisms continue to adapt, rendering them resistant to last-line antibiotics through a complex interplay of anti-carbapenem mechanisms [2,3]. While the mechanisms driving carbapenem resistance vary region-to-region, the most measured and recognized mechanism is carbapenemase production including serine carbapenemases (e.g., *bla*$_{KPC}$) as well as metallo-β-lactamases (MBLs), such as New Delhi metallo-β-lactamase (*bla*$_{NDM}$) [4].

However, the implications of carbapenem resistance occurring in strains which lack a carbapenemase (NCP) has been less studied. NCP related infections have exhibited similar infection-related mortality and healthcare utilization as CPE related infections (5). While carbapenemase-producing Enterobacterales (CPE) is the predominant global driver of CRE, NCPE predominance has been emerging in some regions including South Texas with rates as high as 61% [6,7]. While an increasing rate of clinical laboratories have the capability to detect strains that harbor carbapenemases using currently available molecular rapid diagnostic tests, there is no such test to rapidly detect NCPE strains. This presents a major challenge for timely diagnosis of a CRE infection, leading to delayed targeted treatment, overprescribing of antimicrobials, transmission, and poor outcomes. Moreover, NCPE is attributable to its diverse underlying mechanisms, that most frequently is combinatorial and concerted that cannot be detected by the presence/absence of a specific gene. It is suspected that a higher production of cephalosporinases including extended-spectrum B-lactamase (ESBL) enzymes, like *bla*$_{CTX-M}$, Ambler class C (e.g., *bla*$_{AmpC}$), and certain variants of *bla*$_{SHV}$ contribute to carbapenem resistance among NCP-CRE (4,5). However, additional concerted anti-carbapenem resistance mechanisms with cephalosporinase production such as loss or altered outer membrane protein (Omp) impacting intracellular carbapenem concentration and rate of hydrolysis (level of activity of cephalosporinases) have been implicated and requires further investigation [5].

Moreover, among NCPE are diverse mechanisms including those that are resistant to either meropenem or imipenem-cilastatin but susceptible to ertapenem, adding further complexity to the clinical landscape. The clinical relevance is underscored as the Infectious Diseases Society of America (IDSA) treatment guidelines for gram-negative infections provide specific recommendations for CRE infections which are resistant to ertapenem (MICs ≥ 2 mcg/mL) but susceptible to meropenem (MICs ≤ 1 mcg/mL) (ertapenem-resistant, meropenem susceptible; ErMs) [8]. However, investigations into the molecular and clinical profiles underlying ErMs phenotype have been limited. Previous studies have demonstrated that high levels of ESBL-associated transposon insertional mutagenesis occur in ertapenem resistant *K. pneumoniae* and ST-131 *E. coli* clinical strains, contributing to the evolution of meropenem resistance [9,10]. Consequently, clinicians rely on susceptibility testing results, which can take 3-5 days, before optimizing antibiotics. Herein, we report on mechanisms underlying the phenotypic emergence of ErMs *E. coli* and *K. pneumoniae*, with particular focus on NCPE and those with an ErMs phenotype.

2. Results

2.1. ErMs Predominantly Harbor *bla*$_{CTX-M}$ with *E. coli* Leading the Phenotype among NCPE

As previously reported, 99 CRE isolates from unique patients were collected from 5 hospitals in South Texas, United States between 2011 and 2019 [7]. Of these, E. coli and K. pneumoniae comprised the majority (77%; 76/99), consisting of 47 K. pneumoniae and 29 E. coli. Antimicrobial susceptibility results for E. coli and K. pneumoniae isolates are shown in **Table 1**. Resistance to either ertapenem and/or meropenem was confirmed phenotypically in all isolates. Overall, 38% (29) had an ErMs phenotype while 62% (47) were ertapenem and meropenem resistant (ErMr). E.coli isolates had an ErMs phenotype more frequently than K. pneumoniae (72% v. 17%; $p < 0.001$). Meropenem susceptibilty was maintined by 44% of the CRE isolates. Piperacillin-tazobactam suspectibility was 19% and 35% overall and in ErMs CRE, respectively. Among other common antibiotics active against CRE, susceptibility rates were 77% (ceftazidime-avibactam), 98% (tigecyclin), 16% (levofloxacin), 23% (trimethoprim-sulfamethoxazole), 91% (amikacin), 95% (polymyxins),

and 98% (imipenem-relebactam). Two K. pneumoniae (one NCP-ErMs, one CP-ErMS) and one NCP-E. coli were polymyxin B resistant.

Table 1. Antimicrobial Susceptibilities of Carbapenem Resistant *E. coli* and *K. pneumoniae.*

Name	Overall (%)	ErMs (%)
Amikacin	91	65
Aztreonam	9	12
Ceftazidime-avibactam	77	88
Ciprofloxacin	9	12
Colistin	95	96
Doripenem	53	88
Doxycycline	44	38
Ertapenem	4	0
Cefepime	16	23
Cefotaxime	9	12
Gentamicin	39	48
Imipenem	46	73
Imipenem-relebactam	98	96
Levofloxacin	16	0
Meropenem	44	100
Meropenem-vaborbactam	88	88
Minocycline	63	68
Polymixin B	95	96
Piperacillin-tazobactam	19	35
Trimethoprim-sulfamethoxazole	23	15
Ceftazidime	14	19
Tigecycline	98	96
Ticarcillin-clavulanic acid	11	15
Tobramycin	30	23

Antimicrobial susceptibilities of carbapenem resistant E. coli and K. pneumoniae. Results were collected from medical records and confirmed with microdilution assays (ThermoFisher).

Short-read, whole genome sequence (WGS) analysis was used to annotate known resistance genes among all 76 *E. coli* and *K. pneumoniae* isolates (**Table 2**). Overall, 54% of CRE lacked a carbapenemase gene (NCPE) and 46% (35/76) were CPE. *E. coli* were more frequently NCPE than *K. pneumoniae* (76% v. 40%; $p = 0.01$). Contrastingly, *K. pneumoniae* were more than twice as likely to harbor a carbapenemase gene than *E. coli* (Table 2); predominantly comprised of *bla*$_{KPC}$ (23/28). *K. pneumoniae* also harbored a penicillinase *bla*$_{TEM}$ and/or *bla*$_{SHV}$ more frequently than *E. coli* (89% v. 62%; $p = 0.01$). The ErMs vs. ErMr phenotype were more likely to be NCPE (83% v. 36%, $p < 0.001$) and be enriched for *bla*$_{CTX-M}$ (83% v. 49%, respectively; $p = 0.01$). While CPE were more likely to be ErMr, 5 (14%) of CPE isolates were ErMs, 4 harboring *bla*$_{KPC}$ and one *bla*$_{NDM}$. Contrastingly, ErMr isolates were more commonly CPE than ErMs (64% vs. 17%, $p<0.001$), with *bla*$_{KPC}$ making up the majority of carbapenemase genes among this phenotype (51% vs. 14%, $p = 0.002$). In addition, CP strains carried *bla*$_{OXA-1}$ or *bla*$_{OXA-9}$ more frequently than NCPE strains (60% vs. 29%, $p = 0.01$).

Table 2. Distribution of β-Lactamase Genes by Species, Phenotype, and Carbapenemase Status.

n (%)	Overall (N = 76)	Species			Carbapenem Phenotype			Carbapenemase Status		
		K. pneumoniae (n = 47)	*E. coli* (n = 29)	P-value	ErMr (n = 47)	ErMs (n = 29)	P-Value	CPE (n = 35)	NCPE (n = 41)	P-value
ErMs	29 (38)	8 (17)	21 (72)	**<0.001**				5 (14)	24 (59)	**<0.001**
NCPE	41 (54)	19 (40)	22 (76)	**0.01**	17 (36)	24 (83)	**<0.001**			
CPE	35 (46)	28 (60)	7 (24)	**0.01**	30 (64)	5 (17)	**<0.001**			
***bla*MBL[A]**	5 (7)	3 (6)	2 (7)	1.00	4 (9)	1 (3)	0.70	5 (14)	0 (0)	**0.04**
***bla*KPC[B]**	28 (37)	23 (49)	5 (17)	**0.01**	24 (51)	4 (14)	**0.002**	28 (80)	0 (0)	**<0.001**
***bla*OXA-48[C]**	2 (3)	2 (4)	0 (0)	0.70	2 (4)	0 (0)	0.70	2 (6)	0 (0)	0.41
***bla*OXA-1/-9**	33 (43)	22 (47)	11 (38)	0.60	22 (47)	11 (38)	0.60	21 (60)	12 (29)	**0.01**
***bla*ESBL[D]**	52 (68)	32 (68)	20 (69)	1.00	28 (60)	24 (83)	0.06	21 (60)	31 (76)	0.23
***bla*CTX-M[E]**	47 (62)	27 (57)	20 (69)	0.45	23 (49)	24 (83)	**0.01**	16 (46)	31 (76)	**0.02**
***bla*CTX-M-15**	43 (57)	27 (57)	16 (55)	1.00	22 (47)	21 (72)	**0.05**	16 (46)	27 (66)	0.13
***bla*SHV-12**	7 (9)	7 (15)	0 (0)	0.08	4 (9)	3 (10)	1.00	4 (11)	3 (7)	0.83
***bla*penicillinase[F]**	60 (79)	42 (89)	18 (62)	**0.01**	40 (85)	20 (69)	0.17	30 (86)	30 (73)	0.29
***bla*AmpC[G]**	12 (16)	5 (11)	7 (24)	0.21	7 (15)	5 (17)	1.00	3 (8)	9 (22)	0.20

Distribution of β-lactamase genes based on short-read sequences. **NCPE**: non-carbapenemase producing Enterobacterales, **CPE**: Carbapenemase-producing Enterobacterales, **ESBL**: Extended-spectrum β-lactamase. [A] Metallo-β-lactamases (MBL) variants: *bla*NDM-1, *bla*NDM-5, *bla*VIM-27. [B] *bla*KPC variants: *bla*KPC-2, *bla*KPC-3. [C] *bla*OXA-48-like variants: *bla*OXA-232. [D] ESBL variants: *bla*CTX-M-15, *bla*CTX-M-14, *bla*CTX-M-27, *bla*SHV-12, *bla*SHV-105, *bla*OXY-2-7, *bla*OXY-2-8. [E] Any *bla*CTX-M: *bla*CTX-M-15, *bla*CTX-M-14, *bla*CTX-M-27; [F] *bla*penicillinase: various *bla*TEM-1-like and *bla*SHV-1-like variants. [G] AmpC variants: *bla*CMY-2, *bla*CMY-6, *bla*CMY-42, *bla*CMY-59, *bla*CMY-133, *bla*DHA-9, *bla*FOX-5.

The distribution of MBLs, oxacillinases, AmpC cephalosporinases, and ESBL genes were similar between *E. coli* and *K. pneumoniae*, though *bla*SHV-12 ESBL genes were solely carried by seven *K. pneumoniae* isolates. Five isolates harbored an MBL carbapenemase gene (2 *bla*NDM-1, 2 *bla*NDM-5 and 1 *bla*VIM-27), 28 harbored a *bla*KPC gene (18 *bla*KPC-2, 10 *bla*KPC-3), two harbored a *bla*OXA-232 carbapenemase gene, 33 harbored a narrow spectrum oxacillinase *bla*OXA-1 or *bla*OXA-9 gene (22 *bla*OXA-1, 12 *bla*OXA-9), 52 harbored an ESBL, of which *bla*CTX-M-15 made up the majority (43 *bla*CTX-M-15, 3 *bla*CTX-M-14, 1 *bla*CTX-M-27, 7 *bla*SHV-12, and 1 *bla*SHV-105). *bla*OXA-1 or *bla*OXA-9 was co-harbored with *bla*CTX-M-15 in 27 (36%) of isolates (11 *E. coli* and 16 *K. pneumoniae*). Among *bla*KPC harboring isolates, *bla*OXA-1 or *bla*OXA-9 was co-harbored in 14 (18%) of isolates (3 *E. coli* and 11 *K. pneumoniae*). Sixty (79%) of *E. coli* and *K. pneumoniae* carried a penicillinase gene (*bla*TEM or *bla*SHV). Twelve (16%) *E. coli* and *K. pneumoniae* carried a class C cephalosporinase gene, with plasmid mediated *bla*CMY variants making up the majority (11/12).

2.2. ErMs E. coli Have High Abundance of Mobile Genetic Elements Interposed by blaCTX-M

Mobile genetic elements (MGEs), including insertion sequences (ISs), composite transposons, and other transposable elements are associated with the mobilization of antibiotic resistance genes, including β-lactamases. We aimed to investigate the association between ISs and bla_{CTX-M} genes, particularly their genetic context among ErMs E. coli. To gain insight into MGEs total abundance and MGEs associated with bla_{CTX-M} amplification and mobilization across three distinct carbapenem phenotypes, we annotated MGEs for five bla_{CTX-M} positive ertapenem and meropenem susceptible (ErMs) E. coli, five ErMs E. coli (EC-4, 6, 13, 30, 35), and four ErMr (EC-5, 23, 67, 68) E. coli with MobileElementFinder (https://cge.food.dtu.dk/services/MobileElementFinder/). For this analysis only, clinical EsMs FASTA sequences (Accessions: GCA_032120475.1, GCA_032120375.1, GCA_032122895.1, GCA_032329675.1, GCA_031776215.1) were obtained from NCBI Isolates Browser (https://www.ncbi.nlm.nih.gov/pathogens/isolates#). ErMs and ErMr were selected from our collection to match the various host sources of the EsMs (urine, blood, sputum). To determine bla_{CTX-M} associated MGEs, we included MGEs which were on the same contig and either interposed bla_{CTX-M} or were immediately upstream of bla_{CTX-M}.

ErMs E. coli had higher global mean MGE counts than EsMs (9.4 vs. 0.5, $p < 0.001$) but similar to ErMr strains (**Figure 1a, Supplemental Data S1**). MGEs which were associated with bla_{CTX-M} included IS26, IS26 composite transposon (IS26 inverted repeat flanked unit), ISVsa5 (= IS10R), ISEc9, Tn801, IS102, and ISAs17. Counts of ISAs17 and IS102 were similar in EsMs and ErMs. However, IS26 composite transposon (36.8, $p<0.0001$), IS26 (25.2, $p=0.0006$), Tn801 (23, $p=0.002$), and ISEc9 (17.2, $p=0.03$) mean counts were higher in ErMs than EsMs. Additionally, ISVsa5 was more abundant in ErMs than EsMs and ErMr strains, with over 30 more average ISVsa5 counts than both phenotype groups ($p <0.0001$) (**Figure 1b and 1c**). Comparing ErMs to ErMr showed a wide range of distinct MGEs more abundant in each phenotype (**Supplemental Data S1 and S2**).

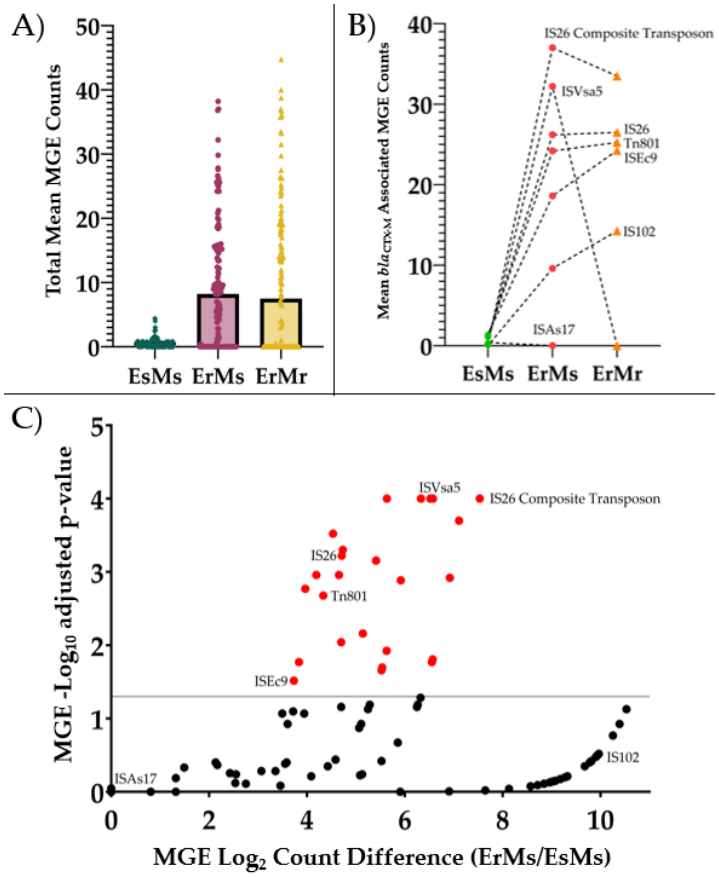

Figure 1. Mean total and bla_{CTX-M} associated mobile genetic elements (MGEs) across three carbapenem phenotypes. Five ertapenem and meropenem susceptible (EsMs) with bla_{CTX-M}, five

ertapenem-resistant but meropenem-susceptible (ErMs), and four ertapenem and meropenem resistant (ErMr) E. coli were annotated for MGEs with MobileElementFinder database v1.0.2 (https://cge.food.dtu.dk/services/MobileElementFinder/). Total annotations counts were compared across all phenotypes (**Figure 1A, Supplemental Data S1**). MGE annotations interposed by (composite transposons) or upstream from $bla_{CTX\text{-}M}$ were counted and plotted across all phenotypes in **Figure 1B**. **Figure 1C** is a volcano plot comparing all MGE counts between EsMs and ErMs. Log2-fold count difference between ErMs and EsMs MGEs were plotted against Log10-transformation adjusted p-values (two way ANOVA) of all MGEs between these two phenotypes. Values above 1.3 Log10 ($p<0.05$; grey line) were considered statistically significant. All red MGEs are present at higher frequencies in ErMs than EsMs E. coli.

2.3. Carbapenemase and $bla_{CTX\text{-}M}$ Hasten Meropenem Hydrolysis in CPE and NCPE

To determine the effect of various β-lactamase profiles on carbapenem hydrolysis rates, intracellular meropenem concentrations were measured through parent molecule quantification over time using liquid chromatography with tandem mass spectrometry (LC-MS-MS). Nine select isolates with diverse profiles were evaluated comprised of isolates harboring bla_{NDM} and bla_{KPC} producing E. coli and K. pneumoniae, and $bla_{CTX\text{-}M\text{-}15}$, $bla_{OXA\text{-}1}$, bla_{TEM} positive non-carbapenemase producing E. coli isolates. Vaborbactam served as a secondary internal standard across all LC-MS-MS assays. The concentration of parent meropenem or vaborbactam molecule (ng/mL) was compared at three time points (1, 2, and 18 hours). Hydrolysis rate was determined using the formula, $\left(-\frac{\Delta[parent]}{\Delta t}\right)$, and reported as ng/mL-hour in **Table 3**. Of the nine isolates, three harbored bla_{NDM} (EC22, EC23, KP26), three harbored bla_{KPC} (EC74, KP15, KP56), and three were NCPE (EC68, EC5, EC201).

Distinct rates of meropenem hydrolysis were observed. Isolates harboring $bla_{CTX\text{-}M}$ displayed higher rates of meropenem hydrolysis across NCPE and CPE isolates (**Table 3**). Those harboring bla_{NDM} showed a dramatic loss of meropenem. Two isolates (EC22 and KP26) rapidly fell below the lower limit of quantitation (LLQ) within one hour while the other isolate (EC23) displayed a rapid rate of meropenem hydrolysis over the over the 18hr experimental period (-2.8 ng/mL-hour). Among the bla_{KPC} harboring isolates (KP56, EC74, and KP15), meropenem hydrolysis was 1.7 times faster, on average, when $bla_{CTX\text{-}M}$ was present (**Table 3**). Among the NCP isolates tested (EC5, EC68 and EC201), the two isolates which harbored $bla_{CTX\text{-}M\text{-}15}$ displayed 1.8 times the meropenem hydrolysis rate as the non-$bla_{CTX\text{-}M\text{-}15}$ isolate (EC68). In fact, the rate of meropenem hydrolysis among the $bla_{CTX\text{-}M\text{-}15}$ positive NCP isolates were similar, and equivalent in the case of EC201, to bla_{KPC} producing isolate KP56 (ATCC 1705). Overall, increased rates of meropenem hydrolysis were primarily driven by carbapenemases but secondarily augmented by the presence of the ESBL $bla_{CTX\text{-}M\text{-}15}$.

Vaborbactam concentrations remained relatively constant over hours 1 and 18 with an average t_2-t_1 concentration of +0.75 (± 1.1) ng/mL and overall average parent (vaborbactam) concentration of 6.0 (± 1.4) ng/mL at all collection time points. No vaborbactam hydrolysis was observed, other than minor loss (-0.1 ng/mL) in EC68 (NCPE) over 18 hours (**Table 3, Supplement Data S2 and S3**).

Table 3. Meropenem Hydrolysis Across Distinct B-lactamase Profiles.

ID	β-Lactamase Profile[A]		Meropenem Hydrolysis (ng/mL-hour)	Vaborbactam Hydrolysis (ng/mL-hour)[B]
	Carbapenemase	Non-Carbapenemase β-Lactamase		
EC68	none	*bla*$_{CMY\text{-}133}$, *bla*$_{TEM\text{-}1}$	-0.5	-0.1
EC5	none	*bla*$_{CTX\text{-}M\text{-}15}$, *bla*$_{OXA\text{-}1}$	-0.8	No loss
EC201	none	*bla*$_{CTX\text{-}M\text{-}15}$, *bla*$_{OXA\text{-}1}$	-1.0	No loss
KP56	*bla*$_{KPC\text{-}2}$	*bla*$_{OXA\text{-}9}$, *bla*$_{TEM\text{-}1}$, *bla*$_{SHV\text{-}182}$	-1.0	No loss
EC74	*bla*$_{KPC\text{-}3}$	none	-1.3	No loss

KP15	*bla*KPC-2	*bla*CTX-M-15, *bla*OXA-9, *bla*TEM-1, *bla*SHV-100	-2.0	No loss
EC23	*bla*NDM-5	*bla*CTX-M-15, *bla*OXA-1, *bla*TEM-1, *bla*SHV-27	-2.8	No loss
EC22	*bla*NDM-5	*bla*CTX-M-15, *bla*OXA-1, *bla*TEM-1, *bla*SHV-27	LLQ at t_1	No loss
KP26	*bla*NDM-1	*bla*CTX-M-15, *bla*CMY-6, *bla*OXA-1, *bla*TEM-1, *bla*SHV-155	LLQ at t_1	No loss

EC: *E. coli*; **KP**: *K. pneumoniae*; **LLQ**: lower limit of quantitation; **None**: none detected; t1: hour 1 since drug exposure; t2: hour 18 since drug exposure. [A] β-lactamase profile determined by short, raw read uploads to ResFinder database [11–13]. [B] Vaborbactam concentrations remained constant between hours 1 and 18 across all nine isolates with an average t_2-t_1 concentration of +0.75 ng/mL and overall average parent concentration of 6.0 ng/mL at all time points.

2.4. Ertapenem Resistant E. coli and K. pneumoniae Carry Elevated Copies of blaCTX-M Genes

The relative copy number (ΔCt) of blaCTX-M, blaOXA-1/9, blaSHV, blaTEM, blaCMY and blaKPC genes were quantified in a subset of eight E. coli and K. pneumoniae ErMs (EC12, EC30, EC31, EC35; KP10, KP38, KP45, and KP54) and eight ceftriaxone-resistant ESBL clinical strains which were ertapenem and meropenem susceptible (EsMs) (EC87, EC88, EC89, EC92; KP85, KP86, KP90, and KP91) (**Table 4**) using quantitative polymerase chain reaction (qPCR). The species specific gene, rpsL, was used as the control gene in both ErMs and EsMs strains. Fold copies were calculated with the formula, $\Delta Ct = 2^{(CTrpsL - CTtarget)}$ relative to rpsL of the same isolate. Overall, the largest copy number difference between the two phenotypes was in blaCTX-M, with a mean difference of 12 fold more $\log_2$-transformed copies in ErMs. The mean difference between all other targeted genes was within one $\log_2$-transformed fold. All blaCTX-M-positive ErMs E. coli (4/4) and K. pneumoniae (3/4) co-harbored blaOXA-1, blaSHV, and/or blaTEM. All ErMs harbored blaTEM, regardless of species. This is in contrast to EsMs, where the majority (5/8) were blaTEM negative. blaSHV was solely harbored by K. pneumoniae, regardless of phenotype. blaCMY was detected at minor levels in one ErMs and two EsMs. blaKPC was detected in two ErMs, EC12 a clinical strain and KP54, an ATCC strain with a distinct subpopulation of KPC producers.

Porin and efflux genes of E. coli (ompC, ompF, tolC) and K. pneumoniae (ompK35, ompK36, oqxA) were also identified and quantified using qPCR relative to rpsL across the same eight ErMs and eight EsMs (**Table 4**). Porin genes were detected in all strains except two K. pneumoniae EsMs which had no detectable ompK35 (KP86 and KP91). Across all tested strains, there was 0.7 fold more $\log_2$-transformed fold copies of porin genes relative to rpsL, ranging from 0.0 to 1.8 fold. Comparing ΔCt of all porins regardless of species, ErMs had more $\log_2$-transformed fold copies than EsMs (0.89x vs. 0.51x; $p = 0.001$). No porin copy number difference was calculated when stratified by species alone. The chromosomal efflux gene of E. coli (tolC) and plasmid efflux gene of K. pneumoniae (oqxA) were also examined with qPCR. All isolates had detectable efflux genes, except KP85. The mean $\log_2$-transformed copies of efflux genes was 0.97, ranging from undetectable to 1.9 fold higher than rpsL.

Table 4. Mean ΔCt of resistance genes relative to *rpsL* among *E. coli* and *K. pneumoniae* ErMs and EsMs.

Phenotype	ID	*rpsL*	*ompC/ompK36*	*ompF/ompK35*	*tolC/oqxA*	*bla*CTX-M	*bla*CMY	*bla*OXA-1/9	*bla*KPC	*bla*SHV	*bla*TEM
ErMs	EC12	1.0	0.5	0.4	0.4	2.3		0.6	1.6		0.4
	EC30		1.4	1.3	1.7	48.8					2.8
	EC31		0.6	0.6	0.8	5.2					0.9
	EC35		0.7	0.9	1.0	39.9	0.1				1.2
	KP10	1.0	0.6	0.7	0.7	10.7		4.3		0.5	4.7
	KP38		1.7	1.8	1.9	20.4				1.6	4.3
	KP45		1.2	1.3	1.0	9.1				9.2	4.9
	KP54		0.2	0.3	0.2			0.2	0.2	0.2	0.2

EsMs	EC87	1.0	0.6	0.5	0.6	1.6		0.7		
	EC88		0.8	0.6	1.9	8.1				
	EC89		0.6	0.7	1.5	2.1				2.0
	EC92		0.5	0.4	1.2	1.4		0.6		
	KP85	1.0	0.5	0.5		1.3		0.5	0.8	1.2
	KP86			0.4	0.6	2.7	0.3		0.7	
	KP90		0.8	1.0	1.6	20		3.6	1.0	8.6
	KP91			0.4	0.4	1.1	0.1			

Mean fold gene copy number relative to *rpsL* (species specific) of ertapenem-resistant but meropenem-susceptible (ErMs) and ceftriaxone-resistant but ertapenem-and-meropenem susceptible (EsMs) *E. coli* and *K. pneumoniae*. Fold copies calculated with formula, $\Delta Ct = 2^{(CTrpsL - CTtarget)}$ relative to each isolate. Group-1 and Group-9 *bla*$_{CTX-M}$ primers used for screening. Porin and efflux genes, ompC/ompF/tolC and ompK35/ompK36/oqxA, were analyzed in *E. coli* and *K. pneumoniae*, respectively. KP54 is ATCC ErMs strain 1903 with a subpopulation of KPC producers.

Based on these data, we quantified the log$_2$-transformed ΔΔCt of bla$_{CTX-M}$ among a larger set of ErMs, using the formula $\Delta\Delta Ct = 2^{(\Delta CTcontrol - \Delta CTtarget)}$. The EsMs E. coli isolate, EC87, was used as the bla$_{CTX-M}$ control strain as it harbored a single copy of bla$_{CTX-M}$ relative to rpsL with a log2 ΔΔCt of zero. We examined 16 ErMs E. coli (**Table 6**), six ErMs K. pneumoniae, four EsMs E. coli and four EsMs K. pneumoniae. Overall, 82% (18) of the 22 ErMs harbored bla$_{CTX-M-15}$ or bla$_{CTX-M-14}$, while the four remaining ErMs had no detectable bla$_{CTX-M}$ (**Figure 2)**. Furthermore, ErMs isolates harboring bla$_{CTX-M}$ carried 4-fold more log$_2$-transformed copies of bla$_{CTX-M}$ than ceftriaxone-resistant EsMs (3.7 v. 0.9, $p < 0.001$) across both species and carbapenemase status. Interestingly, NCP-ErMs had 3-fold more bla$_{CTX-M}$ copies than CP-ErMs (4.0 vs. 0.8) (**Figure 2**).

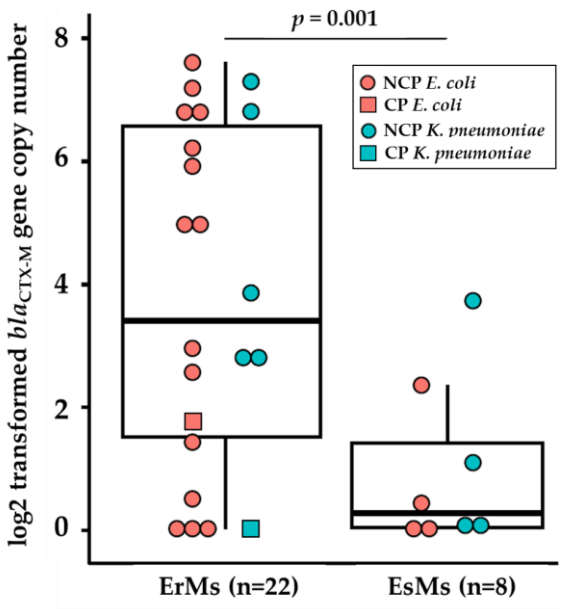

Figure 2. Mean log$_2$-transformed bla$_{CTX-M}$ gene copy number by ertapenem and meropenem phenotype. $\Delta\Delta Ct = 2^{(\Delta CTcontrol - \Delta CTtarget)}$ was used to calculate copy number, using rpsL gene as the control gene and EC87 (a ceftriaxone-resistant but ertapenem and meropenem susceptible (EsMs) strain) as the control strain (bla$_{CTX-M}$ ΔCt of 1.0; log2 ΔΔCt = 0.0). **Abbreviations**: **bla**: β-lactamase; **EsMs**: ertapenem-and-meropenem susceptible but ceftriaxone-resistant; **ErMs**: ertapenem-resistant, meropenem susceptible. Performed t-test for fold change difference between ErMs and EsMs.

2.5. ompC Frameshifts are Frequent Among Ertapenem Resistant NCPE E. coli

Though minimal differences in porin gene copy numbers were observed between ErMs vs. EsMs, sequence mutations outside of the qPCR primer sequence may be present at different rates. In order to examine this, we aligned short-read sequences to a reference genome, *Escherichia coli* str. K-12 substr. MG1655 (GenBank Accession: U00096) and *K. pneumoniae* CP000647. Porin gene alterations were then translated and categorized into three major amino acid variant categories, including 1) insertions and/or deletions, 2) frameshifts, or 3) premature stops.

Amino acid variants in *ompF*-like (*ompF*/*ompK35*) and *ompC*-like (*ompC*/*ompK36*) porin genes in CP-ErMr and NCP-ErMs *E. coli* and *K. pneumoniae* isolates are summarized in **Table 5**. Results were stratified by species as distinct porin alteration rates occur between *E. coli* vs. *K. pneumoniae*, requiring separate analysis. All eight (100%) of ErMs *K. pneumoniae* were NCP while 76% (16/21) of the *E. coli* ErMs were NCP and 24% (5/21) of *E. coli* ErMs harbored bla_{KPC-2}, bla_{KPC-3}, or bla_{NDM-5}.

Overall, porin variants were not detected in 100% and 3.6% of CP-ErMr *E. coli* and *K. pneumoniae*. A translated amino acid alteration from either *ompC* or *ompF* sequences was significantly more frequent in NCP-ErMs *E. coli* than CP-ErMr *E. coli* (p = 0.002). Contrastingly, translated porin gene alterations were both more frequent and similar in alteration type (insertion/deletion, frameshift, premature stop) in NCP-ErMs vs. CP-ErMr *K. pneumoniae* isolates, regardless of porin gene type (*ompK35* or *ompK36*).

In *K. pneumoniae*, premature stop codons in *ompK35* or *ompK36* genes occurred in 89% and 100% of CP-ErMr and NCP-ErMs isolates with similar rates in individual porin genes. The most frequent premature stop codon positions in *ompK35* porin genes were p213* and p89*, occurring in 30% and 26% of all *K. pneumoniae* isolates. In *ompK36* genes, p271* was the most frequent position of a premature stop codon. Concurrent *ompK35* and *ompK36* premature stop codons occurred in 57% (27/47) of all *K. pneumoniae* isolates. In addition, insertion/deletion (indel) and frameshift alterations occurred at similar rates in *ompK36* genes, regardless of carbapenemase status and phenotype. This is in opposition to *ompK35*, which was free of any indels or frameshifts among CP-ErMr and NCP-ErMs *K. pneumoniae* (**Table 5**).

Among NCP-ErMs *E. coli*, frameshift alterations were significantly more frequent than CP-ErMs *E. coli* (100% v. 0%; p = 0.002), with frameshifts being detected in *ompC* or *ompF* in 88% and 50% of NCP-ErMs *E. coli*, respectively. *ompC* or *ompF* indels occurred in 63% of NCP-ErMs *E. coli* and none of the CP-ErMr *E. coli*. A premature stop codon was detected in one *E. coli*, which occurred in the *ompC* gene of a NCP-ErMs isolate.

In addition to these major translated porin gene alterations (indel, frameshift, premature stop), translated missense amino acid changes were mapped to the protein databank (PDB) coordinate files of OmpF, OmpC, OmpK35, and OmpK36 (PDB: 4GCS, 7JZ3, 5o77, 6RD3). The non-synonymous residue alterations predominantly related to external facing vestibular loops, including Loop 3, within OmpC/OmpK36 and OmpF/OmpK35 (**Supplemental Data S2)**. In addition, frameshift mutations occurred most frequently within the Loop 4-β8-Loop 5 extracellular facing vestibule region, primarily in NCPE isolates. Of note, a GG, PT, or the previously reported GGD insertion within the conserved Loop 3 region (amino acid positions 133-136) of OmpK36 occurred solely among the high-risk *Klebsiella pneumoniae* clones 258 and 307, while *E. coli* Loop 3 nucleotides contained various missense changes only.

Table 5. Major Amino Acid Alterations in Porin Genes in *E. coli* and *K. pneumoniae* by Carbapenemase Status and Carbapenem Phenotype.

	E. coli			***K. pneumoniae***		
	CP-ErMr (n = 2)	**NCP-ErMs (n = 16)**	**P-value**	**CP-ErMr (n = 28)**	**NCP-ErMs (n = 8)**	**P-value**
No major alteration(s)	2 (100)	0 (0)	**0.002**	1 (3.6)	0 (0)	1.00
Any major alteration(s)	0 (0)	16 (100)	**0.002**	27 (96)	8 (100)	1.00

ompC/ompK35	0 (0)	14 (88)	**0.05**	27 (96)	8 (100)	1.00
ompF/ompK36	0 (0)	8 (50)	0.55	20 (71)	4 (50)	0.47
Insertion/Deletion	0 (0)	10 (63)	0.85	27 (96)	8 (100)	1.00
ompC/ompK35	0 (0)	10 (63)	0.85	27 (96)	8 (100)	1.00
ompF/ompK36	0 (0)	0 (0)	ND	0 (0)	0 (0)	ND
Frameshift	0 (0)	16 (100)	**0.002**	27 (96)	8 (100)	1.00
ompC/ompK35	0 (0)	14 (88)	**0.05**	24 (85)	8 (100)	0.62
ompF/ompK36	0 (0)	8 (50)	0.55	0 (0)	0 (0)	ND
Premature Stop	0 (0)	1 (6.2)	1.00	25 (89)	8 (100)	0.80
ompC/ompK35	0 (0)	1 (6.2)	1.00	23 (82)	7 (87)	1.00
ompF/ompK36	0 (0)	0 (0)	ND	20 (71)	4 (50)	0.47

Major amino acid alterations in porin genes in *E. coli* and *K. pneumoniae* by carbapenemase status and carbapenem phenotype determined by short-read sequences mapped to reference. Abbreviations: **CP**: carbapenemase-producing; **ErMs**: ertapenem-resistant, meropenem-susceptible; **ErMr**: ertapenem and meropenem resistant; **NCP**: non-carbapenemase producing; **ND**: not detected. [A] Major alterations in either *ompF*-like or *ompC*-like genes are included unless specific gene noted.

Overall, the frequency and type of translated porin alterations among ErMr and ErMs K. pneumoniae was not different, which was in contrast to NCP-ErMs E. coli. As ertapenem resistance seems to be related to ompC alterations, among NCP-ErMs E. coli specifically, further genomic analysis was warranted. Coverage of the ompC gene was assessed in 26 E. coli (20 NCP, 6 CP) by viewing the mapped reads coverage and annotating low coverage areas, defined as areas where coverage falls below two standard deviations from the mean coverage (**Supplemental Data S2, S4** and **Table 6**). Of the E. coli genomes visualized, 62% (16/26) had a no-to-low read coverage region within the ompC gene averaging 103 ± 61 bp long, ranging from 7 bp to 173 bp in length across all visualized genomes. MG1655 K12 E. coli was used as mapping reference; accession: U00096 (Nucleotide [Internet]. Bethesda (MD): National Library of Medicine (US), National Center for Biotechnology Information; [1988] - [cited 2023 Nov 11]. Available from: https://www.ncbi.nlm.nih.gov/nuccore/U00096.2).

ompC lesions were highly similar among all strains, spanning from c.416 - c.554, with c.531 occuring at the terminal end of the gap in 50% of sequences. NCP-E. coli represented 77% (20/26) of the visualized sequences and made up 94% (15/16) of the sequences with ompC coverage gaps. ErMs and ErMr made up 81% (13/16) and 19% (3/16) of these ompC lesioned strains, respectively. Despite this, ompC alignment gaps among ErMs (13/21) vs. ErMr (3/5) E. coli was not significantly different. Of the 10 strains that had complete ompC coverage (no hits on the low coverage annotation track) (EC-4, 12, 13, 14, 22, 23, 29, 67, 69, 75), the majority were CP (60%) comprised of one CP-ErMr (EC23) and five CP-ErMs (EC-12, 13, 14, 22, 75). No ompC lesions were noted in four NCP E. coli (EC-4, 29, 67, 69). Overall, this highlights a distinct ompC genomic structure among CP vs. NCP E. coli. The lack of ompC lesions among vizualied CP-E. coli (100%), regardless of bla_{KPC} (4/10) or bla_{NDM} (2/10), compared to only 20% (4/20) of NCP-E. coli indicates an important role of ompC genetic disruption among NCP E. coli ($p < 0.001$) independent of ertapenem resistance.

2.6. Ertapenem Resistant E. coli Lack OmpC Outer Membrane Protein

Though ompC genetic lesions seem to be related to E. coli's carbapenemase status rather than carbapenem phenotype, the level of OmpC protein expression among ErMs is unknown. To examine OmpC outer membrane protein abundance among ErMs, we used sodium dodecyl sulfate–polyacrylamide gel electrophoresis (SDS-PAGE) and immunodetection with anti-OmpC and anti-OmpF primary antibodies (ThermoFisher). Major porin OmpC presence/absence was evaluated in a subset of 16 representative ErMs E. coli isolates with four EsMs E. coli as OmpC control strains (EC87, 88, 89 and 92). These EsMs

clinical strains were used as controls as they carried qPCR confirmed bla_{CTX-M} yet remained ertapenem susceptible. Four of the ErMs isolates were CP-ErMs E. coli (3 bla_{KPC-2}, 1 bla_{KPC-3}) while 12 were NCP-ErMs E. coli. See **Table 6** for a summary of genomic and immunodetection results.

All four control EsMs had detectable OmpC bands (**Figure 3a**). OmpC was not detected in 81% (13/16) of tested ErMs E. coli. The three lanes in which OmpC was detected were loaded with EC12, EC14, and EC75, which are all bla_{KPC} producing ErMs E. coli. In fact, 75% (3/4) of the electrophoretically separated CP-ErMs E. coli lysates had a detectable OmpC band. Furthermore, the one CP-ErMs which did not have a detectable OmpC band (EC13) had 5-fold more genetic copies of $bla_{CTX-M-15}$ than EsMs controls which is 5x more copies than the other CP-ErMs (**Table 6**). NCP-ErMs E. coli made up 75% (12/16) of the samples tested for OmpC separation (EC-2, 3, 4, 6, 30, 31, 32, 33, 34, 35, 36, 66). No OmpC band was detected in any of these samples.

A combination of anti-OmpF and anti-OmpC primary antibodies (multiplexed) were used on a selection of nine ErMs E. coli and ATCC 2340 (**Figure 3b**). It is evident that a band below OmpC (40 kDa) and around 37 kDa was visible in 6/9 of the isolates (EC2, EC13, EC30, EC31, EC32, EC33). However, the other three isolates (ATCC 2340, EC12, EC22, and EC69) had very strong signals despite protein concentration normalization, making OmpC/F distinction difficult to interpret.

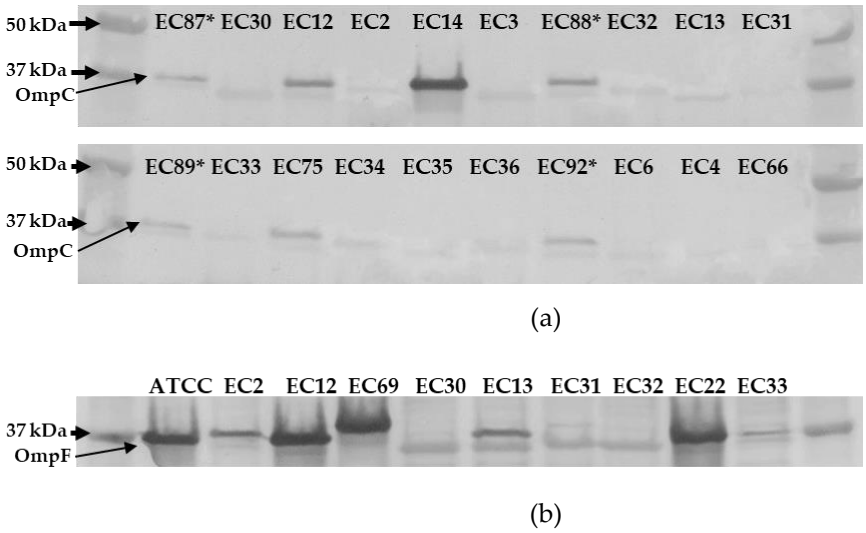

Figure 3. Immunodetection of OmpC in ertapenem-resistant *E. coli* clinical strains grown in Mueller Hinton broth overnight. Total proteins were resolved by 4-15% SDS-PAGE. The proteins were electro-transferred to nitrocellulose membrane and immunodetected with polyclonal antibody directed against denatured OmpC and/or OmpF porins. Only the relevant part of the blot is shown. Isolates EC87*, EC88*, EC89*, and EC92* are ertapenem-susceptible, ceftriaxone-resistant (EsMs) *E. coli* clinical isolates. ATCC 2340 was used as positive control. **(a)** Immunodetection of OmpC in ertapenem-resistant, meropenem susceptible (ErMs) *E. coli* clinical strains. Thick black arrows indicate molecular weights, thin black arrows indicate the region of OmpC. **(b)** Immunodetection of OmpF and OmpC in ErMs *E. coli* clinical strains. Thick black arrows indicate molecular weight, thin black arrows indicate the region of OmpF.

Table 6. Summary of ErMs E. coli bla_{CTX-M} copy number, ompC contig coverage and OmpC status.

ID	Carbapenemase Status	bla_{CTX-M} ΔΔCt[A]	Contig Coverage[B] at K12 *ompC*	OmpC Band[C]
EC12	CP (bla_{KPC})	+ 1.7	**No gap** (Full coverage)	Detected
EC14	CP (bla_{KPC})	+ 0.5	**No gap** (Low at c.539 – c.545)	Detected

EC13	CP (*bla*KPC)	+ 5.0	**No gap** (Full coverage)	ND
EC75	CP (*bla*KPC)	ND	**No gap** (Full coverage)	Detected
EC30	NCP	+ 6.2	**149 bp gap** (c.424 - c.531)	ND
EC31	NCP	+ 2.9	**29 bp gap** (c.544 – c.531)	ND
EC35	NCP	+ 5.9	**144 bp gap** (c.429 – c.531)	ND
EC2	NCP	+ 4.9	**149 bp gap** (c.424 – c.531)	ND
EC3	NCP	+ 6.6	**173 bp gap** (c.416 – c.515)	ND
EC32	NCP	+ 1.4	**150 bp gap** (c.424 – c.530)	ND
EC33	NCP	+ 7.5	**149 bp gap** (c.424 – c.530)	ND
EC34	NCP	ND	**139 bp gap**[D] (c.434 – c.531)	ND
EC36	NCP	+ 7.1	**140 bp gap** (c.434 – c.530)	ND
EC4	NCP	+ 6.8	**No gap** (Full coverage)	ND
EC6	NCP	+ 2.5	**141 bp gap** (c.431 – c.532)	ND
EC66	NCP	ND	**149 bp gap** (c.424 – c.531)	ND

Summary of ErMs E. coli blaCTX-M copy number variations, ompC mapped reads coverage and OmpC expression status. **A)** $\Delta\Delta Ct = 2^{(CTcontrol - CTtarget)}$ was used to calculate copy number, using rpsL gene as the control. **B)** Contigs were de novo assembled, dissolved, and mapped to K12 (accession: U00096). If multiple gaps were detected, the largest was reported. **C)** Total protein was prepared as a lysate, normalized, electrophoretically seperated on a 4-15% gel and detected with anti-OmpC rabbit antibodies (**Figure 3a**). **D)** In addition to the noted ompC gap, EC34 had a 5,570 bp gap spanning from c.343 of ompC to adjacent genes downstream. **Abbreviations**: **BP**: base pair; **CP**: carbapenemase producing; **NCP**: non-carbapenamse producing; **ND**: not detected.

3. Discussion

To thwart potential mistreatment of patients inflicted with NCPE and/or ErMs CRE infections, more insight into the anti-carbapenem resistance mechanisms employed by these nefarious pathogens is urgently needed. This is especially true for infectious diseases caused by ErMs **—a phenotype with significant clinical implications**. This study revealed that ErMs E. coli genomes contain more total MGEs counts than EsMs (**Figure 1a**), particularly blaCTX-M associated MGEs, including IS26, IS26 composite transposon, ISVsa5 (= IS10R), ISEc9, and Tn801 (**Figure 1b-c**). These MGEs were found to be either interposed by or directly adjacent to blaCTX-M in ErMs E. coli. IS26 is recognized for its frequent mobilization of antimicrobial resistance genes as "translocatable units," inserting them adjacent to other IS26 copies in gram-negative bacteria. The blaCTX-M genes are often associated with IS26-interrupted transposable elements positioned upstream from ISVSa5, synonymous with IS10R, the active element in the plasmid-associated transposon Tn10. Moreover, IS10R has demonstrated internal promoter regions in previous work [31]. As ISVSa5 were significantly more abundant in ErMs than EsMs and ErMr strains, this

insertion sequence could be significant in regulating bla_{CTX-M} expression in ErMs E. coli. Additionally, qualitative results of bla_{CTX-M} (presence/absence) in patient samples may be insufficient - rather it is necessary to quantify the number of copies harbored by E. coli and K. pneumoniae as elevated copies can relate to ertapenem resistance (**Figure 2**). This is in contrast to carbapenemases, where determining the presence/absence of the gene seems to be sufficient to relate to ertapenem resistance as single copies were able to produce ertapenem and meropenem resistance efficiently. In conjunction with this, OmpC loss is evidently critical for the development of the ErMs phenotype, as 75% of ErMr and 100% of EsMs but none of the ErMs isolates maintained OmpC (**Figure 3a**). Additionally, all bla_{KPC} producers with a single bla_{CTX-M} copy had detectable OmpC bands but when multiple bla_{CTX-M} copies were detected (5-fold more than EsMs) no OmpC was detected (EC13) (**Figure 3a, Table 6**). Taken together, this provides compelling evidence that a collaborative effort between bla_{CTX-M} and OmpC occurs to result in ertapenem but not meropenem resistance and NCP E. coli (**Figure 4**). As bla_{CTX-M} seems to be a less efficient carbapenem hydrolyzing enzyme than bla_{KPC} and bla_{NDM} (**Table 4**), insertion sequence disruption or other events may be triggered to disrupt OmpC expression. As ompC genomic lesions were more associated with carbapenemase status than ertapenem phenotype, it is more likely that the ErMs phenotype is an outcome of transcriptional or translational regulation. Another related potential cause of OmpC loss among the 16 E. coli ErMs immunoblotted (**Figure 3**) is that 50% (8/16) of the isolates came from urinary sources (**Supplement Data S2**) and seven out of those eight (88%) had no detectable OmpC. Previous literature has demonstrated that high osmolarity can cause transcriptional downregulation of outer membrane proteins through the envZ/OmpR system [14,15]. However, in these environments, OmpF tends to be more labile than OmpC. Loss of OmpF seems to be less critical for the development of ErMs E. coli as the majority maintained a visible OmpF band (**Figure 3b**).

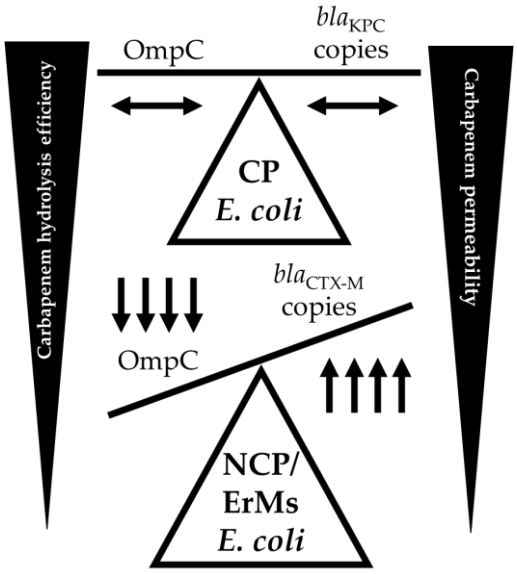

Figure 4. Diagram depicting the balance between carbapenem hydrolysis efficiency of β-lactamases and OmpC expression (present/absent) among carbapenemase producing (CP), non-carbapenemase producing (NCP), and ertapenem resistant, meropenem susceptible (ErMs) E. coli. As carbapenemase enzymes, like bla_{KPC}, are harbored in E. coli, OmpC expression is maintained in the presence of carbapenem exposure. However, if bla_{CTX-M} is present in NCP E. coli, carbapenem exposure drives an increase in bla_{CTX-M} copies and a decrease in OmpC expression.

Within this CRE collection, E. coli were NCPE and/or had an ErMs phenotype more frequently than K. pneumoniae (**Table 2**). The fact that 72% (21/29) of the collected E. coli displayed an ErMs phenotype poses a great risk to patient care, as the ertapenem

phenotype is selectively "hidden" or not reported in an effort to reduce ertapenem use in our local hospitals. Not reporting ertapenem phenotype may lead to mistreatment of patients infected with this CRE subtype. As ESBL producing Enterobacterales (ESBL-E) are on the rise in our area and globally, it may be prudent to test and report ertapenem results along with reduce the use of cephalosporins, like ceftriaxone, to possibly foil the rise of bla_{CTX-M} copy number variant ErMs strains. K. pneumoniae were more commonly carbapenemase producing, with bla_{KPC} being the most prevalent carbapenemase among the species (**Table 2**). In addition, bla_{SHV} and bla_{TEM} genes were amidst K. pneumoniae genomes more frequently than E. coli genomes. $bla_{OXA-1/9}$ genes were also more commonly associated with CPE than NCPE. These co-harbored β-lactamase genes have been reported previously and seem to mobilize on modular genomic elements regularly [16,17]. In addition, $bla_{OXA-1/9}$ have been previously associated with piperacillin-tazobactam resistance [10,17], which was reflected among this collection. Specifically, 22/29 (76%) of all ErMs were piperacillin-tazobactam resistant and 10/12 (83%) of the $bla_{OXA-1/9}$ positive ErMs were piperacillin-tazobactam resistant. All $bla_{OXA-1/9}$ positive ErMs co-harbored $bla_{CTX-M-15}$.

These data also provide insight into the enzymatic efficiency of β-lactamases across the Ambler classes. A pattern of increased hydrolysis was measured in pathogens harboring bla_{CTX-M}, bla_{KPC}, and bla_{NDM}. Excluding isolates which co-harbored any two of these three enzymes, an average meropenem hydrolysis rate was (-0.9 ng/mL-hour) for bla_{CTX-M} positive isolates and (-1.2 ng/mL-hour) for bla_{KPC} positive isolates; a 1.3 times increase in hydrolysis in bla_{KPC} vs. bla_{CTX-M} carrying isolates. All bla_{NDM} positive isolates co-harbored bla_{CTX-M}, with two of these isolates achieving loss of meropenem below the lower limit of quantitation (LLQ) within the first hour. Examining the three NCPE tested isolates, a 1.8 times increase of meropenem hydrolysis was measured in bla_{CTX-M} (EC5 and EC201) vs. non-bla_{CTX-M} (EC68) carrying isolate(s). These data may require the cononical attribution of "non-carbapenemase" to be reconsidered for bla_{CTX-M} positive isolates, as bla_{CTX-M} copy number variant strains can result in carbapenem hydrolysis and resistance. Another interesting finding in this analysis was the slight average increase of 0.75 (± 1.1) ng/mL/18 hours in vaborbactam across all nine isolates. This may be related to a recycling or reversed binding of parent substrate [vaborbactam] as the total number of replicating isolates, and the β-lactamases they produced, decreased over time.

In order to apply these findings to future work, it is important to consider the limitations associated with this study. Though we hypothesis that OmpC loss seems to be driven by genetic lesions which result in coverage gaps within the mid-range of the gene, this phenomenon can occur from many biological or environmental mechanisms, including mobile genetic element mediated disruption of ompC [10] and osmolarity. In addition, depending on the reference genome used to map contigs against, difference coverage scores could be seen. When reviewing the multiplexed immublot (**Figure 3b**), the primary antibodies used may have some cross reactivity due to similarity of epitopes, however, when used alone (**Figure 3a**), the molecular weights aid in qualitative analysis of the bands. In terms of LC-MS/MS assays, β-lactams are very labile chemicals as they are prone to hydrolyzation unless stringent protocols are followed. Because of this, meropenem hydrolysis results may have been susceptible to non-β-lactamase degredation. It was attempted to control for by nulling out baseline hydrolysis of parent molecule. Also, the contribution of a single β-lactamase is difficult in clinical isolates which harbor multiple classes of β-lactamases without working with isogenic strains. Also, since β-lactamase copy number was not calculated in these nine isolates, it is unclear if increased copies of these genes effected the meropenem hydrolysis rates, though most studies do not determine copy number variation of β-lactamase genes. In terms of clinically relevant limitations, the fact that a large portion of the collected CRE were from urinary sources makes extrapolation to non-urinary infections difficult.

In conclusion, we used short read, whole genomic data in conjunction with LC-MS/MS, qPCR and western blotting techniques to provide molecular characterization of NCPE and ErMs E. coli and K. pneumoniae. The ErMs phenotype seems to be related to

elevated gene copies of $bla_{CTX\text{-}M\text{-}14}$ and $bla_{CTX\text{-}M\text{-}15}$, especially when concurrently present with ompC genetic lesions and loss of OmpC production. Loss of OmpF seems to be less critical for the development of ErMs E. coli. Future efforts to characterize the molecular mechanisms which promote OmpC loss and quantification of $bla_{CTX\text{-}M}$ among CRE will potentially improve patient care and mitigate further expansion of ertapenem resistance among patients afflicted with E. coli and/or K. pneumoniae infections.

4. Materials and Methods

4.1. Bacterial Isolates and Antimicrobial Susceptibility Testing

Carbapenem-resistant E. coli (n = 29) and K. pneumoniae (n = 47) isolates were examined from a previously collected biorepository of 99 CRE from 85 unique patients admitted to five different hospitals in South Texas, USA between 2011 and 2019. Clinical isolates were stored at the time of carbapenem-resistance discovery following Clinical and Laboratory Standards Institute (CLSI) standards and clinical laboratory procedures (e.g., positive Modified Hodge test, rapid antimicrobial resistance gene detection). All isolates were initially speciated through biochemical assays and/or mass spectrometry at the clinical laboratory. Repeat confirmatory speciation was determined through WGS-KMER analysis. Abiding by current CDC definitions, CRE in this study were defined as Enterobacterales isolates resistant to any carbapenem or determined to be carbapenemase positive. The in-vivo sources of the isolates varied (**Supplement Data S2**). MICs of the isolates at the time of patient hospitalization were abstracted from electronic medical records and confirmed with microdilution susceptibility testing using the Sensititre™ Gram Negative GNX2F AST Plate. Discrepencies in phenotypes were present among a small number of isolates (~2%), which were primariliy K. pneumoniae and were interpreted as ErMs in the medical chart but ErMr upon repeat testing. These isolates were annotated as ErMr in downstream analysis. Carbapenem non-susceptibility was defined based on CLSI breakpoints: ertapenem-and-meropenem susceptible but ceftriaxone-resistant (EsMs): ertapenem ≤ 0.5 mcg/mL, meropenem MIC ≤ 1 mcg/mL and ceftriaxone MIC ≥ 4 mcg/mL; ErMs: ertapenem ≥1 mcg/mL and meropenem MIC ≤ 1 mcg/mL (ertapenem intermediate breakpoint annotated as resistant); ertapenem-and-meropenem resistant (ErMr): ertapenem ≥ 2 mcg/mL and meropenem MIC ≥ 4 mcg/mL (CLSI M100, ED33). CRE with carbapenemase genes detected were termed CPE; those without carbapenemase genes were termed NCPE. E. coli strains ATCC 25922 and BAA-2340 were used as carbapenem-susceptible and carbapenem-resistant (bla_{KPC} producing) controls, respectively. Klebsiella pneumoniae strains BAA-1705, BAA-1706 and BAA-1903 were used as bla_{KPC}-producing, non-carbapenemase producing and ErMs controls, respectively.

4.2. Whole Genome Sequencing

For WGS, total bacterial DNA was extracted with DNeasy PowerSoil kit (Qiagen). For qPCR, genomic and plasmidic DNA were extracted by following the CDC boil Bac-DNA Lysate protocol. WGS was conducted on all isolates using a NextSeq 500 sequencing instrument (Illumina Inc., San Diego, CA) with 150-base paired-end reads (UT Health San Antonio, San Antonio, TX). All short-read data and metadata have been deposited in the NCBI BioProject (PRJNA1049776). De-novo assembly, variant analyses and contig coverage visualization were conducted using CLC Genomics Workbench 20.1 (Qiagen, Redwood City, CA) and Geneious Prime® 2023.1.2. For assigning bacterial species, multilocus sequence typing (MLST) was performed using KmerFinder Database version 3.0.2 [18–20] and MLST 2.0 [21–27]. The identification of antimicrobial resistance genes and point mutations in CRE isolates was accomplished through the use of PointFinder and ResFinder version 4.1 [11–13]. Core genome alignments were generated through alignment of short-read sequences to reference genome, Escherichia coli str. K-12 substr. MG1655 (GenBank Accession: U00096) and K. pneumoniae CP000647. OmpC, OmpF, OmpK35, and OmpK36 amino acid changes were visualized and mapped to tertiary protein databank structures

(7JZ3, 4GCS, 5o77, 6RD3) using the molecular graphics program, VMD [28]. ompC coverage gaps for all 29 E. coli Illumina paired-end-read files were trimmed, merged, normalized and de novo assembled into contigs. Assembled contig lists of all 29 E. coli resulted in an average N50 of 59,489 base pairs (bp) long and an average sum contig length of 7,355,703 bp. Other assembly features are summarized in **Supplement Data S2 and S4**. Contig lists were dissolved and mapped against MG1655 K12 E. coli reference genome (accession: U00096).

4.3. Immunodetection and Sample Preperation

Samples from overnight growth in CAMH broth with ertapenem (1 ug/mL) were pelleted and solubilized in 200 uL water. Cell lysis was then accomplished through three rounds of freeze-thaw cycles, sonication and boiling at 100 °C for 8 minutes. Bacterial protein lysate concentrations were determined with BCA Protein Assay Kit (Pierce) and samples were normalized to 1.2 ug/mL then separated by electrophoresis with BIO-RAD Mini-PROTEAN TGX Stain-Free Gels with 4-15% polyacrylamide for an hour at 150V. Bands were transferred onto nitrocellulose membranes at 25V for 50 minutes. Membranes were then blocked with 1% gelatin in 1x transfer buffer solution with tween (TBST) and anti-OmpC or anti-OmpF antibodies (ThermoFisher) overnight at 4°C on a shaker. The membrane was then washed three times with ddH2O and subjected to a secondary antibody reaction with the BioRad Immuno-Blot Assay Kit (Goat anti-rabbit IgG) by diluting goat anti-rabbit secondary antibodies in gelatin buffer solution and rocking at 20°C for 60 minutes. Membranes were washed three times with TBST solution and developed alkaline phosphatase.

In an effort to understand osmolarity related effects on porin band intensity on included isolates, representative CRE clinical strains were grown in three different broths, ranging in osmolarity, including high salt Luria-Bertani Miller (LB) Millers broth (highest osmolarity), cation-adjusted Mueller-Hinton (CAMH) (low-moderate osmolarity), and nutrient broth (low osmolarity). No differences were seen in OmpC or OmpF bands between media, including in the ATCC reference strains (**Supplement Data S2**). Thus, CAMH was used solely for currently reported experiments. Four ertapenem and meropenem susceptible (EsMs) but ceftriaxone resistant E. coli clinical isolates collected from blood sources were used as OmpC controls (**Figure 3**). In addition, ATCC 2340, a meropenem-resistant, bla_{KPC} producing CLSI control strain, was used as the reference for porin protein bands.

4.4. qPCR of β-lactamase genes

To determine gene copy numbers, SYBR Green qPCR was performed using primers and a microplate reader (BioRad). Copy number was calculated using the formula $\Delta Ct = 2^{(CTcontrol - CTtarget)}$ and the mean plate Cq value for rpsL as the control gene [10,29]. Primers used for qPCR included a $bla_{CTX\text{-}M\text{-}15}$ specific primer: 5′- ATGGATGAAAGGCAATACCA-3′ with an estimated amplicon size of 175 nucleotides (this study). In addition, a Group-1 $bla_{CTX\text{-}M}$ primer: 5′-ATGGTTAAAAAATCACTGCG-3′ and Group-9 $bla_{CTX\text{-}M}$ primer: 5′-ATGGTGACAAAGAGAGTGCA-3′ were used to both capture any addition $bla_{CTX\text{-}M}$ genes within the groups as well as $bla_{CTX\text{-}M\text{-}14}$ within Group-9 [30]. A bla_{KPC} primer was also used to screen ErMs isolates: 5′-TGTCACTGTATCGCCGTCTA-3′ (this study). Other primers included $bla_{OXA\text{-}1}$: 5′- ACGTGGATGCAATTTTCTGT-3′ (this study), bla_{SHV}: 5′-GCCGCTTGAGCAAATTAAAC-3′ (this study), bla_{TEM}: 5′-CTGTTTTTGCTCACCCAGAA-3′ (this study), E. coli rpsL: 5′-ACCACCGATGTAGGAAGTCA-3′ (this study), and K. pneumoniae rpsL: 5′-GACCTTCACCACCGATGTAG-3′ (this study). All performed equally well with 100% agreement with WGS data.

4.5. Sample Preparation for LC-MS/MS Analysis

The bacterial strains were grown on tryptic soy agar (TSA) with 5% sheep blood for 24 hours at 37°C. A single bacterial isolate was transferred to cation adjusted Muller Hinton broth (CA-MHB). The cultures were incubated and shaken for 18 hours. At the end of incubation, an (OD_{600}) MacFarland 0.5 standard concentration was prepared with each inoculum. A meropenem-vaborbactam E-TEST strip (MEV [64/8 ug/mL]) was placed into a volume of 0.8 mL CA-MHB then shaken for 30 minutes at 37°C. Standardized inoculum was then transferred (0.2mL) to each meropenem-vaborbactam-concentrated broth and incubated while shaken. At hours 1, 4 and 18, a 0.2 mL sample volume collection was taken from the test samples and centrifuged at 12,000 RPM at 4°C for 10 minutes. At the end of the centrifugation, 100 uL volume of the resulting supernatant was collected and transfer to 300 uL ice cold methanol and 15uL of internal standard propranolol (IS) to a concentration of 5 ug/mL. Each tube was lightly vortex by hand for 0.2 minutes then placed on ice to incubate for 10 minutes. The remaining volume of the supernatant for each bacterial sample was carefully removed and the resulting bacterial cell pellets were resuspended in 100 uL of PBS pH 7.4, sonicated for 5 minutes and then were processed as were the collected 100 uL supernatant samples noted above for protein precipitation and pellet sample analysis. After ice incubation, samples were mixed then centrifuged at 12,000 g at 4°C for 10 minutes. A 100 uL volume of the supernatant was then transferred to 200 uL HPLC-grade water and mixed briefly. Sample was then transferred (150 uL) to a LC-MS/MS sample injection vial for analysis. Ertapenem and imipenem proved to be too labile to accurately detect at concentrations less than 128 mcg/mL. Meropenem remained stable at lower concentrations (< 10 ng/mL). The sample analysis of the abundance of meropenem, inhibitor vaborbactam and the selected (IS) internal standard propranolol were measured using a LC-MS/MS system comprising of a ACQUITY UPLC liquid chromatogram system and a Xevo TQD, tandem triple-quadrupole mass spectrometer by Waters corporation. Additional instrumentation parameters and analysis can be found in the supplemental information.

4.6. Statistical Analyses

The Student's t test or the nonparametric Wilcoxon Rank Sum test was used for continuous variables based on distribution. The chi-square or Fisher's Exact test was used to compare categorical variables. A two-sided p-value of less than 0.05 was considered statistically significant. All analyses were completed with R (v4.1.2) statistical program/packages.

Supplementary Materials: The following supporting information can be downloaded at: www.mdpi.com/xxx/s1, **Supplemental Data S1**: annotated mobile genetic elements and counts of included ErMs and EsMs; **Supplemental Data S2**: ErMs vs. ErMr mobile genetic element count volcano plot, OmpC alteration sites on modeled structure, SDS-PAGE and immunodetection results, LC-MS/MS analysis concentrations at time points, Standard curve and quality control/sample preparation for LC-MS/MS analysis, *In-vivo* sources of collected ErMs *E. coli* and *K. pneumoniae* isolates, Distribution of porin amino acid alterations among *E. coli* and *Klebsiella* spp., Mapped reads of ErMs *E. coli* (EC30) with coverage gap in *ompC*; **Supplemental Data S3**: LC-MS/MS standard curve and parent molecule concentration calculations; **Supplemental Data S4:** Contig details of assembled ErMs *E. coli* used for *ompC* mapping.

Author Contributions: CAB: conceptualization. CAB and GCL: analyses and draft the manuscript. CB, RB, SB, SA, and KQ: data extraction and experimentation. CB, GL, SD, GG, and WS: data interpretation. RB, SB, SD, GG, WS, SA, DS, KR, CF, JK, NW, and AM: provide edits. All authors contributed to the article and approved the submitted version.

Funding: This study was supported in part by Merck. Data was generated in the Genome Sequencing Facility, which is supported by UT Health San Antonio, NIH-NCI P30 CA054174 (Cancer Center at UT Health San Antonio), NIH Shared Instrument grant 1S10OD021805-01 (S10 grant), and CPRIT Core Facility Award (RP160732). CAB was participating in a Translational Science Training T32 program (1T32TR004544-01) and was also partially supported by the National Center for Advancing Translational Sciences, National Institutes of Health, through Grant UL1TR002645, while he

performed this work. GCL was supported by the National Institutes of Aging (NIA/NIH K23-AG066933). The views expressed in this article are those of the authors and do not necessarily represent the views of Merck, Department of Veterans Affairs, the National Institutes of Health, or the authors' affiliated institutions.

Institutional Review Board Statement: This study was approved by the institutional review board of the University of Texas Health at San Antonio with a waiver of informed consent.

Informed Consent Statement: Informed consent was waived due to the retrospective nature of the study.

Data Availability Statement: Data supporting results have been deposited in the NCBI BioProject (PRJNA1049776).

Conflicts of Interest: Authors declare no conflicts of interest.

References

1. World Health Organization Implementation Manual to Prevent and Control the Spread of Carbapenem-Resistant Organisms at the National and Health Care Facility Level: Interim Practical Manual Supporting Implementation of the Guidelines for the Prevention and Control of Carbapenem-Resistant Enterobacteriaceae, Acinetobacter Baumannii and Pseudomonas Aeruginosa in Health Care Facilities; World Health Organization, 2019;
2. Lasko, M.J.; Nicolau, D.P. Carbapenem-Resistant Enterobacterales: Considerations for Treatment in the Era of New Antimicrobials and Evolving Enzymology. *Curr Infect Dis Rep* **2020**, *22*, 6, doi:10.1007/s11908-020-0716-3.
3. Tracking CRE in the United States| HAI | CDC Available online: https://www.cdc.gov/hai/organisms/cre/trackingcre.html (accessed on 31 January 2023).
4. Karlsson, M.; Lutgring, J.D.; Ansari, U.; Lawsin, A.; Albrecht, V.; McAllister, G.; Daniels, J.; Lonsway, D.; McKay, S.; Beldavs, Z.; et al. Molecular Characterization of Carbapenem-Resistant Enterobacterales Collected in the United States. *Microb Drug Resist* **2022**, *28*, 389–397, doi:10.1089/mdr.2021.0106.
5. Lee, Y.Q.; Sri La Sri Ponnampalavanar, S.; Chong, C.W.; Karunakaran, R.; Vellasamy, K.M.; Abdul Jabar, K.; Kong, Z.X.; Lau, M.Y.; Teh, C.S.J. Characterisation of Non-Carbapenemase-Producing Carbapenem-Resistant Klebsiella Pneumoniae Based on Their Clinical and Molecular Profile in Malaysia. *Antibiotics (Basel)* **2022**, *11*, 1670, doi:10.3390/antibiotics11111670.
6. Chea, N.; Bulens, S.N.; Kongphet-Tran, T.; Lynfield, R.; Shaw, K.M.; Vagnone, P.S.; Kainer, M.A.; Muleta, D.B.; Wilson, L.; Vaeth, E.; et al. Improved Phenotype-Based Definition for Identifying Carbapenemase Producers among Carbapenem-Resistant Enterobacteriaceae. *Emerg Infect Dis* **2015**, *21*, 1611–1616, doi:10.3201/eid2109.150198.
7. Black, C.A.; So, W.; Dallas, S.S.; Gawrys, G.; Benavides, R.; Aguilar, S.; Chen, C.-J.; Shurko, J.F.; Lee, G.C. Predominance of Non-Carbapenemase Producing Carbapenem-Resistant Enterobacterales in South Texas. *Front. Microbiol.* **2021**, *11*, doi:10.3389/fmicb.2020.623574.
8. Tamma PD, Aitken SL, Bonomo RA, Mathers AJ, van Duin D, Clancy CJ. Infectious Diseases Society of America Antimicrobial-Resistant Treatment Guidance: Gram-Negative Bacterial Infections. Infectious Diseases Society of America 2023; Version 3.0. Available at https://www.idsociety.org/practice-guideline/amr-guidance/. Accessed 12/09/2023.
9. Ma, P.; He, L.L.; Pironti, A.; Laibinis, H.H.; Ernst, C.M.; Manson, A.L.; Bhattacharyya, R.P.; Earl, A.M.; Livny, J.; Hung, D.T. Genetic Determinants Facilitating the Evolution of Resistance to Carbapenem Antibiotics. *eLife* **2021**, *10*, e67310, doi:10.7554/eLife.67310.
10. Shropshire, W.C.; Aitken, S.L.; Pifer, R.; Kim, J.; Bhatti, M.M.; Li, X.; Kalia, A.; Galloway-Peña, J.; Sahasrabhojane, P.; Arias, C.A.; et al. IS26-Mediated Amplification of blaOXA-1 and blaCTX-M-15 with Concurrent Outer Membrane Porin Disruption Associated with de Novo Carbapenem Resistance in a Recurrent Bacteraemia Cohort. *Journal of Antimicrobial Chemotherapy* **2021**, *76*, 385–395, doi:10.1093/jac/dkaa447.
11. Zankari, E.; Allesøe, R.; Joensen, K.G.; Cavaco, L.M.; Lund, O.; Aarestrup, F.M. PointFinder: A Novel Web Tool for WGS-Based Detection of Antimicrobial Resistance Associated with Chromosomal Point Mutations in Bacterial Pathogens. *J Antimicrob Chemother* **2017**, *72*, 2764–2768, doi:10.1093/jac/dkx217.
12. Bortolaia, V.; Kaas, R.S.; Ruppe, E.; Roberts, M.C.; Schwarz, S.; Cattoir, V.; Philippon, A.; Allesoe, R.L.; Rebelo, A.R.; Florensa, A.F.; et al. ResFinder 4.0 for Predictions of Phenotypes from Genotypes. *J Antimicrob Chemother* **2020**, *75*, 3491–3500, doi:10.1093/jac/dkaa345.
13. Clausen, P.T.L.C.; Aarestrup, F.M.; Lund, O. Rapid and Precise Alignment of Raw Reads against Redundant Databases with KMA. *BMC Bioinformatics* **2018**, *19*, 307, doi:10.1186/s12859-018-2336-6.
14. Pinet, E.; Franceschi, C.; Davin-Regli, A.; Zambardi, G.; Pagès, J.-M. 2015 Role of the Culture Medium in Porin Expression and Piperacillin-Tazobactam Susceptibility in Escherichia Coli. *Journal of Medical Microbiology 64*, 1305–1314, doi:10.1099/jmm.0.000152.
15. Boxtel, R. van; Wattel, A.A.; Arenas, J.; Goessens, W.H.F.; Tommassen, J. Acquisition of Carbapenem Resistance by Plasmid-Encoded-AmpC-Expressing Escherichia Coli. *Antimicrobial Agents and Chemotherapy* **2017**, *61*, doi:10.1128/AAC.01413-16.

16. Shropshire, W.C.; Dinh, A.Q.; Earley, M.; Komarow, L.; Panesso, D.; Rydell, K.; Gómez-Villegas, S.I.; Miao, H.; Hill, C.; Chen, L.; et al. Accessory Genomes Drive Independent Spread of Carbapenem-Resistant Klebsiella Pneumoniae Clonal Groups 258 and 307 in Houston, TX. *mBio* **2022**, *13*, e00497-22, doi:10.1128/mbio.00497-22.
17. Livermore, D.M.; Day, M.; Cleary, P.; Hopkins, K.L.; Toleman, M.A.; Wareham, D.W.; Wiuff, C.; Doumith, M.; Woodford, N. OXA-1 β-Lactamase and Non-Susceptibility to Penicillin/β-Lactamase Inhibitor Combinations among ESBL-Producing Escherichia Coli. *Journal of Antimicrobial Chemotherapy* **2019**, *74*, 326–333, doi:10.1093/jac/dky453.
18. Hasman, H.; Saputra, D.; Sicheritz-Ponten, T.; Lund, O.; Svendsen, C.A.; Frimodt-Møller, N.; Aarestrup, F.M. Rapid Whole-Genome Sequencing for Detection and Characterization of Microorganisms Directly from Clinical Samples. *J Clin Microbiol* **2014**, *52*, 139–146, doi:10.1128/JCM.02452-13.
19. Larsen, M.V.; Cosentino, S.; Lukjancenko, O.; Saputra, D.; Rasmussen, S.; Hasman, H.; Sicheritz-Pontén, T.; Aarestrup, F.M.; Ussery, D.W.; Lund, O. Benchmarking of Methods for Genomic Taxonomy. *J Clin Microbiol* **2014**, *52*, 1529–1539, doi:10.1128/JCM.02981-13.
20. Clausen, P.T.L.C.; Aarestrup, F.M.; Lund, O. Rapid and Precise Alignment of Raw Reads against Redundant Databases with KMA. *BMC Bioinformatics* **2018**, *19*, 307, doi:10.1186/s12859-018-2336-6.
21. Larsen, M.V.; Cosentino, S.; Rasmussen, S.; Friis, C.; Hasman, H.; Marvig, R.L.; Jelsbak, L.; Sicheritz-Pontén, T.; Ussery, D.W.; Aarestrup, F.M.; et al. Multilocus Sequence Typing of Total-Genome-Sequenced Bacteria. *J Clin Microbiol* **2012**, *50*, 1355–1361, doi:10.1128/JCM.06094-11.
22. Bartual, S.G.; Seifert, H.; Hippler, C.; Luzon, M.A.D.; Wisplinghoff, H.; Rodríguez-Valera, F. Development of a Multilocus Sequence Typing Scheme for Characterization of Clinical Isolates of Acinetobacter Baumannii. *J Clin Microbiol* **2005**, *43*, 4382–4390, doi:10.1128/JCM.43.9.4382-4390.2005.
23. Griffiths, D.; Fawley, W.; Kachrimanidou, M.; Bowden, R.; Crook, D.W.; Fung, R.; Golubchik, T.; Harding, R.M.; Jeffery, K.J.M.; Jolley, K.A.; et al. Multilocus Sequence Typing of Clostridium Difficile. *J Clin Microbiol* **2010**, *48*, 770–778, doi:10.1128/JCM.01796-09.
24. Lemee, L.; Dhalluin, A.; Pestel-Caron, M.; Lemeland, J.-F.; Pons, J.-L. Multilocus Sequence Typing Analysis of Human and Animal Clostridium Difficile Isolates of Various Toxigenic Types. *J Clin Microbiol* **2004**, *42*, 2609–2617, doi:10.1128/JCM.42.6.2609-2617.2004.
25. Wirth, T.; Falush, D.; Lan, R.; Colles, F.; Mensa, P.; Wieler, L.H.; Karch, H.; Reeves, P.R.; Maiden, M.C.J.; Ochman, H.; et al. Sex and Virulence in Escherichia Coli: An Evolutionary Perspective. *Mol Microbiol* **2006**, *60*, 1136–1151, doi:10.1111/j.1365-2958.2006.05172.x.
26. Jaureguy, F.; Landraud, L.; Passet, V.; Diancourt, L.; Frapy, E.; Guigon, G.; Carbonnelle, E.; Lortholary, O.; Clermont, O.; Denamur, E.; et al. Phylogenetic and Genomic Diversity of Human Bacteremic Escherichia Coli Strains. *BMC Genomics* **2008**, *9*, 560, doi:10.1186/1471-2164-9-560.
27. Camacho, C.; Coulouris, G.; Avagyan, V.; Ma, N.; Papadopoulos, J.; Bealer, K.; Madden, T.L. BLAST+: Architecture and Applications. *BMC Bioinformatics* **2009**, *10*, 421, doi:10.1186/1471-2105-10-421.
28. Humphrey, W.; Dalke, A.; Schulten, K. VMD: Visual Molecular Dynamics. *Journal of Molecular Graphics* **1996**, *14*, 33–38, doi:10.1016/0263-7855(96)00018-5.
29. Adler, M.; Anjum, M.; Andersson, D.I.; Sandegren, L. Influence of Acquired β-Lactamases on the Evolution of Spontaneous Carbapenem Resistance in Escherichia Coli. *Journal of Antimicrobial Chemotherapy* **2013**, *68*, 51–59, doi:10.1093/jac/dks368.
30. Rivoarilala, O.L.; Garin, B.; Andriamahery, F.; Collard, J.M. Rapid in Vitro Detection of CTX-M Groups 1, 2, 8, 9 Resistance Genes by LAMP Assays. *PLoS One* **2018**, *13*, e0200421, doi:10.1371/journal.pone.0200421.
31. Martínez-García, E.; Navarro-Lloréns, J.M.; Tormo, A. Identification of an Unknown Promoter, OUTIIp, within the IS10R Element. *J Bacteriol* **2003**, *185*, 2046-50. doi: 10.1128/JB.185.6.2046-2050.2003.